

A Simplified Means for Computation of Interconnect Distributed Capacitances and Inductances

George L. Matthaei, *Life Fellow, IEEE*, Gilbert C. Chinn, Charles H. Plott, *Member, IEEE*, and Nadir Dagli, *Member, IEEE*

Abstract—A simplified, approximate means for computing the distributed capacitance and inductance matrices for TEM-mode (or quasi-TEM-mode) single or multiple transmission lines is presented. Cases having multiple dielectrics and/or ground planes are included. The conductors used may be either rectangular or planar. Simplicity is achieved by use of the “method of moments” along with two physically meaningful charge basis functions per conductor face. The techniques utilized are relatively easy to program and result in fast programs which are accurate for many important geometries. Such programs should be suitable for inclusion as subroutines in larger CAD programs for analysis and design of high-speed digital or microwave circuits.

I. INTRODUCTION

THE purpose of this paper is to present approximate means for computing interconnect parameters that are sufficiently simple and fast that they can readily be incorporated as a subroutine in a CAD program for the design of high-speed digital or microwave circuits. The concepts and equations involved in the methods described below are sufficiently simple that most engineers will have little difficulty in relatively quickly writing their own program based on them. The methods used involve approximations which tend to lose accuracy in some unlikely situations such as the case of two coplanar strips with an extremely small separation. However, as will be illustrated by examples, in the practical range of line geometries the accuracy is surprisingly high.

Existing programs for treating problems of this type typically involve the “method of moments” in some form [1]–[3], often using a large number of rectangular or other charge basis functions, or a finite-element method using a very large number of elements [4], [5]. These approaches are quite general and can be very accurate, but they may require the generation and inversion of large matrices, two processes which can lead to considerable program complexity and a large amount of computation.

Manuscript received November 5, 1990. This work was supported by DARPA under Office of Naval Research Contract N00014-88-K-0497. This paper was recommended by Associate Editor D. Scharfetter.

G. L. Matthaei, G. C. Chinn, and N. Dagli are with the Department of Electrical and Computer Engineering, University of California, Santa Barbara, CA 93106.

C. H. Plott was with the Department of Electrical and Computer Engineering, University of California, Santa Barbara. He is now with the Hewlett Packard Company, Santa Rosa, CA 95403.

IEEE Log Number 9105720.

(Sometimes the matrix size to be inverted may be of the order of hundreds or even thousands.) Here we also use the method of moments but, instead, use two kinds of physically meaningful charge basis functions, each of which is associated with an entire side of a conductor. In this way there are only two basis functions used per side of a rectangular conductor, and the required matrix size is only two times the number of sides that must be represented. This approach, however, does have the limitation that only planar, rectangular, or possibly trapezoidal conductors can be considered. However, this is not a drawback for most situations of practical interest. Our method also uses “point matching” in the method of moments (which implies the use of delta-function “testing” functions). This also adds simplicity to our procedures.

We will first consider the problem of computing the interconnect capacitances per unit length. After having established procedures for doing this, the computation of the corresponding inductances per unit length will be quite simple.

II. THE CHARGE BASIS FUNCTIONS

Fig. 1(a) shows a flat conductor of width w which extends to infinity into and out of the paper. One of the two basic charge distribution functions we use is the even-symmetric function

$$\sigma_e(x, b, w) = \frac{q}{\sqrt{(w/2)^2 - (x - b)^2}} \Big|_{|x-b| \leq w/2} \quad (1)$$

which is sketched in Fig. 1(b). This charge distribution is exactly that which would occur on an infinitely thin conductor such as that in Fig. 1(a) if there were charge q coulombs/meter along the length of the conductor and an equal amount of opposite charge at infinity [6]. It can be shown [6] that the potential arising from (1) observed at any point $z = x + jy$ in the complex plane is given by

$$\phi_e(z, b, w) = q \left[\frac{1}{\epsilon_0} H_e(z, w, b) \right] \quad (2a)$$

where

$$H_e(z, b, w) = \left(-\frac{1}{2\pi} \right) \text{Im} \left[\arcsin \left(\frac{z - b}{w/2} \right) \right]. \quad (2b)$$

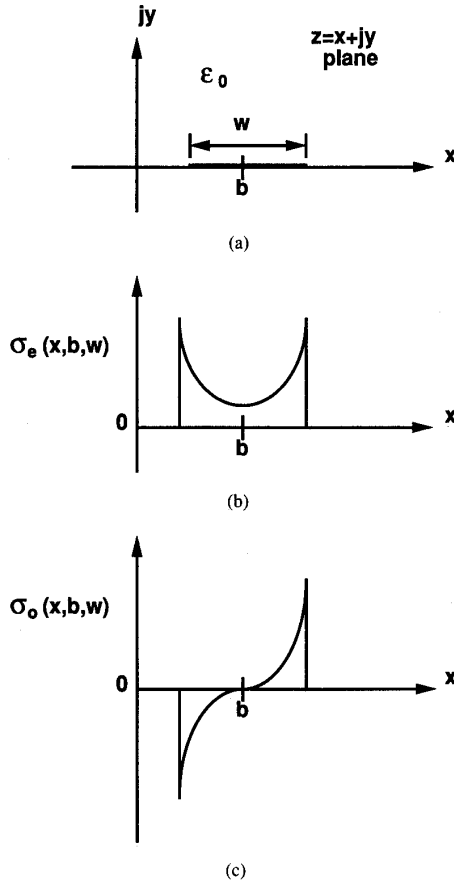


Fig. 1. (a) A metal strip which extends into and out of the paper. (b) An even charge basis function such as is used in this paper. (c) The corresponding odd basis function.

Here, ϵ_0 is the dielectric constant of the medium, b locates the center of the charge distribution of width w , and, in general, b can be complex so as to center the charge distribution anywhere in the plane. An even-symmetric charge basis function as used herein will consist of a charge distribution as in (1) at a surface of the conductor plus any images of this charge that may be required by the presence of dielectric or metal planar interfaces (as will be explained Sections IV and V below).

We also use the corresponding odd-symmetric charge distribution

$$\sigma_o(x, b, w) = \frac{A(x-b)}{\sqrt{(w/2)^2 - (x-b)^2}} \Big|_{|x-b| \leq w/2} \quad (3)$$

which is sketched in Fig. 1(c). This is the charge distribution function that would be induced on the conductor in Fig. 1(a) if it were immersed in a uniform electric field in the x direction in the figure. We have determined that the potential at any z caused by the charge distribution (3) centered at b is given by

$$\phi_o(z, b, w) = g \left[\frac{1}{\epsilon_0} H_o(z, w, b) \right] \quad (4a)$$

where

$$H_o(z, b, w) = \text{Re} [(z-b) - \text{sign}(\text{Re}(z-b)) \cdot \sqrt{(z-b)^2 - (w/2)^2}] \quad (4b)$$

Here $\text{sign}(\cdot)$ is to be replaced by the sign of its argument. The constant g in (4a) is either π times A in (3) or something close to that value. However, we have not concerned ourselves with this point because it will be convenient to simply deal with g in (4a), and the relation between A and g is not required. Note that the distribution in (3) has zero net charge. The odd-symmetric charge basis functions that we use consist of a distribution as in (3) at a surface of the conductor plus any images of this charge that may be needed to represent the effects of adjacent dielectric or metal interfaces.

In the methods below we use a superposition of the above even and odd charge distributions to approximate the charge distribution on each face of a conductor. Examples have shown that in most instances this works very well. However the use of these distributions can be seen to have one weakness in that in the case of rectangular conductors they contain a charge singularity at the corners which is somewhat stronger than it should be. It is known that the transverse field and charge singularity as one approaches the edge of an infinitely thin conductor as in Fig. 1(a) should blow up according to $\rho^{-1/2}$, where ρ is the distance from the edge of the strip [7]. Equations (1) and (3) are seen to have this property. However, in the case of a right-angle corner, the charge distribution should blow up according to $\rho^{-1/3}$ [7]. Thus, particularly in the case of rectangular conductors, we will wish to keep the sampling points for potential away from the corners since the charge and potential there will be somewhat excessive.

III. A SIMPLE EXAMPLE

The main concepts of the method are easily explained in terms of a simple example, which we will refer to as Example 1. Consider the problem of obtaining the distributed capacitance between symmetrical coplanar strips as in Fig. 2, which are viewed as extending into and out of the paper and which have negligible thickness. For the moment let us assume that $\epsilon_1 = \epsilon_0$. We apply potential V and $-V$ to the strips as shown, and represent the total charge distribution on each strip by the sum of an even distribution as in (1) plus an odd distribution as given by (3). The potentials at any point z arising from these distributions are given by (2a), (2b), (4a), and (4b) and they sum to

$$\begin{aligned} \phi(z) = & Q[H_e(z, b, w) - H_e(z, -b, w)] \\ & + G[H_o(z, b, w) + H_o(z, -b, w)] \end{aligned} \quad (5)$$

where

$$Q = q/\epsilon_0 \quad \text{and} \quad G = g/\epsilon_0. \quad (6)$$

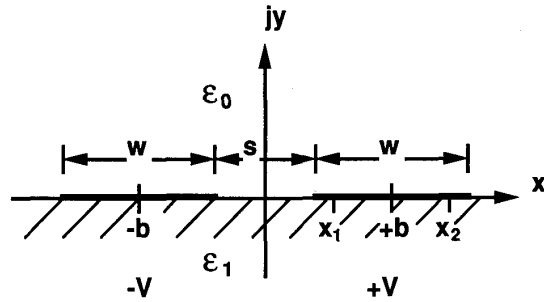


Fig. 2. Two coplanar strips extending into and out of the paper.

Q is the normalized charge per unit length and G is the normalized odd-distribution amplitude. Implicit in (5) is the fact that since the potential on the left strip is the negative of that on the right strip, the same relation applies between the charge distributions on the two strips. For this reason the $H_e(z, -b, w)$ for the left strip has the opposite sign to $H_e(z, b, w)$ for the right strip. However, note that $H_o(z, -b, w)$ has the same sign as $H_o(z, b, w)$ for the right strip since it can be seen that if an odd charge distribution as in Fig. 1(c) is simply translated to the left to be centered at $x = -b$, the resulting distribution at $x = -b$ will be the negative of the original distribution at $x = b$. Thus the plus sign is correct for the second square bracket in (5).

For simplicity we will rewrite (5) as

$$\phi(z) = Qh_e(z) + Gh_o(z). \quad (7)$$

Note that because of the symmetry in this particular problem we only need to solve for two amplitudes Q and G in order to completely define our approximate charge distributions. We will do this by forcing the potential $\phi(z)$ to be equal to V at the two match points

$$\begin{aligned} z_1 = x_1 &= b - (r)w/2 \\ z_2 = x_2 &= b + (r)w/2 \end{aligned} \quad (8)$$

indicated in Fig. 2. Here we have introduced a match-point parameter r , which is the ratio of the distance of a match point from the center of a charge distribution divided by the half-width of the distribution. (We have found that for either thick or thin conductors where there is no ground plane nearby $r = 0.8$ is a good value to use.) These constraints lead to the equations

$$\begin{bmatrix} h_e(x_1) & h_o(x_1) \\ h_e(x_2) & h_o(x_2) \end{bmatrix} \begin{bmatrix} Q \\ G \end{bmatrix} = \begin{bmatrix} -V \\ V \end{bmatrix} \quad (9)$$

which are readily solved for Q and G . Then the capacitance per unit length between the strips is

$$C = q/(2V) = \epsilon_0 Q/(2V). \quad (10)$$

Note that though G was a necessary part of the solution, it is not used in computing C since the odd charge basis function has zero net charge.

TABLE I
THE NORMALIZED DISTRIBUTED CAPACITANCE FOR COPLANAR STRIPS AS IN FIG. 2 COMPUTED BY THE METHODS OF THIS PAPER, COMPARED WITH EXACT VALUES

s/w	C/ϵ_0^*	% Error [†]	s/w	C/ϵ_0^*	% Error [†]
0.1	2.808	-0.43	0.5	1.910	0.47
0.2	2.423	0.62	1.0	1.567	0.26
0.3	2.191	0.64	2.0	1.280	0.08
0.4	2.031	0.59	3.0	1.140	0.00

* Computed by methods of this paper for uniform dielectric ϵ_0 .

† Percent error compared with results computed from conformal mapping.

In Table I values C/ϵ_0 are tabulated for this example as computed by the above methods and also as computed from an exact formula [8]. The percentage error is also given. Note that the accuracy is excellent, even for the case where s/w is only 0.1.

In Fig. 2 the coplanar strips are shown to be on a substrate with dielectric constant ϵ_1 . That case can easily be handled by the above analysis because adding dielectric to the lower half plane will have no effect on the electric field pattern, though it will increase the D field in the lower half plane by the relative dielectric constant. Thus if ϵ_1 differs from ϵ_0 the distributed capacitance between the strips becomes

$$C' = \left(\frac{\epsilon_1 + \epsilon_0}{2} \right) \left(\frac{C}{\epsilon_0} \right) \quad (11)$$

where C was for $\epsilon_1 = \epsilon_0$.

IV. FORMULATION OF CASES INVOLVING RECTANGULAR CONDUCTORS

Let us now consider the more general case of two asymmetric rectangular conductors on a dielectric substrate. Our discussion also is applicable to cases including additional conductors. Here we will also need the potentials $U_e(z_k, b_m, w_m)$ and $U_o(z_k, b_m, w_m)$ at any point z_k caused by vertically oriented even- and odd-charge basis functions of the forms in (1) and (3). Their potential functions are easily defined in terms of (2b) and (4b) to be

$$U_e(z_k, b_m, w_m) = H_e(-jz_k, -jb_m, w_m) \quad (12)$$

and

$$U_o(z_k, b_m, w_m) = H_o(-jz_k, -jb_m, w_m). \quad (13)$$

Here b_m is a complex number which locates the center of the m th conductor face and w_m defines the width of that face.

In the example in Fig. 3 we have followed a convention in numbering the faces which we have found to be convenient for programming purposes. Going from left to right, we first number the bottom faces of the two conductors plus the bottom faces of any additional conductors which might be included on the right. (Note that the z_k and the b_k are both defined using this convention.) If the

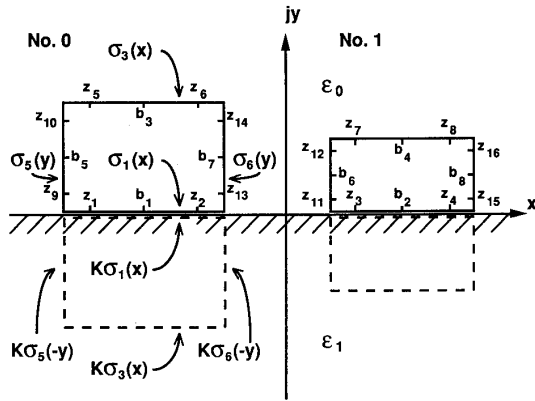


Fig. 3. A pair of asymmetrical thick conductors on a semi-infinite dielectric substrate.

problem deals with very thin conductors these will be the only faces that need to be used. If accounting for conductor thickness is desired, then starting from the left we next number all the horizontal faces at the tops of the conductors. Next we add numbering on the vertical faces. A convenient scheme is first to number the left faces of all the strips going from left to right and then to number the right faces in the same manner. Using this numbering scheme for the b_m and z_k points, it is easy to provide user options for including charge distributions only for the conductors' bottoms, or for the bottoms, tops, and sides, as may be desirable for a given situation. Also the numbers m for the various faces of a given strip will always differ by a multiple of M , the number of strips.

In the case in Fig. 3 we include image charge distributions (suggested by dashed lines in the figure) to account for the effects of the dielectric interface. Then with the images in place the problem is solved using only the dielectric constant ϵ_0 for the upper region. As suggested in the figure, the image charges are of exactly the same form as the charges in the upper region except they are scaled in amplitude by [9]

$$K = \frac{\epsilon_0 - \epsilon_1}{\epsilon_0 + \epsilon_1}. \quad (14)$$

Note that if $\epsilon_1 > \epsilon_0$, then K will be negative so that the sign of the image charge in the lower half plane will be the opposite of that for charge at the corresponding point in the upper half plane. Including the image, the potential from a horizontal even-symmetric basis function for a conductor face centered at b_m is seen to be

$$P_{km}^e = [H_e(z_k, b_m, w_m) + KH_e(z_k, \bar{b}_m, w_m)] \quad (15a)$$

while that from a vertical even-symmetric basis function is

$$P_{km}^e = [U_e(z_k, b_m, w_m) + KU_e(\bar{z}_k, b_m, w_m)]. \quad (15b)$$

Here \bar{z}_k and \bar{b}_m are the complex conjugates of z_k and b_m . Likewise, the potential from an odd-symmetric basis function for a horizontal conductor face is

$$P_{km}^o = [H_o(z_k, b_m, w_m) + KH_o(z_k, \bar{b}_m, w_m)] \quad (16a)$$

while that for a vertical conductor face is

$$P_{km}^o = [U_o(z_k, b_m, w_m) + KU_o(\bar{z}_k, b_m, w_m)]. \quad (16b)$$

(The different use of conjugates in (15a) and (16a) as compared with (15b) and (16b) is necessary to provide the proper symmetry.) We have degrees of freedom to fix the potential at two points on each conductor face, and these "match points" can be defined for a horizontal conductor face m by

$$z_{2m-1} = b_m - (rh)w_m/2 \quad z_{2m} = b_m + (rh)w_m/2 \quad (17a)$$

and for vertical face m by

$$z_{2m-1} = b_m - j(rv)w_m/2 \quad z_{2m} = b_m + j(rv)w_m/2. \quad (17b)$$

Here the parameters rh and rv have the same significance as r in (8) but for flexibility they have been defined independently for the horizontal and vertical faces, respectively. Though the solution is usually not very sensitive to the precise value of rh and rv , we have found that expect for an extreme situation or two, which will be noted in Section X, $rh = rv = 0.8$ are particularly good values to use if the structure has no ground plane, and $rh = 0.67$ with $rv = 0.8$ are particularly good to use if the structure has a ground plane (or two).

Let us assume that the configuration to be analyzed has M thick conductors, so we want to include charge on all four faces of each conductor. Then, analogous to (5) and (9), using (15a), (15b), (16a), and (16b), we obtain the system of equations

$$\sum_{m=1}^{4M} P_{km}^e Q_m + P_{km}^o G_m = v_k |_{k=1 \text{ to } 8M} \quad (18a)$$

or

$$\begin{bmatrix} P^e & P^o \end{bmatrix} \begin{bmatrix} Q \\ G \end{bmatrix} = [v]. \quad (18b)$$

In the above the v_k are the potentials at the $8M$ match points z_k , while the P^e and P^o are both matrices with $8M$ rows and $4M$ columns. Thus (18b) contains an $8M$ by $8M$ matrix (formed from P^e and P^o) multiplied by a vector consisting of $4M$ unknown Q_m values and $4M$ unknown G_m values (defined as in (6)). Of course, if the strips are thin the number of equations can be reduced to $2M$, as discussed above, since only one pair of basis functions will be required per strip. We shall discuss the fixing of the v_k values in the next two sections.

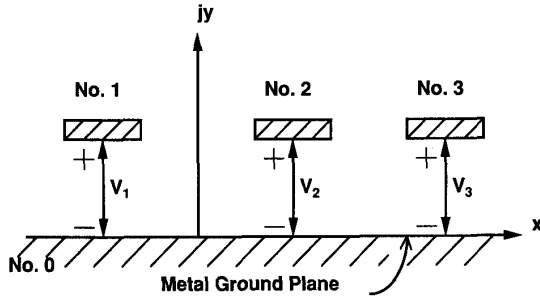


Fig. 4. Three transmission-line conductors with their voltages referred to a ground plane.

V. CALCULATION OF THE CAPACITANCE MATRIX WHEN THE VOLTAGES ARE REFERENCED TO A GROUND PLANE

Let us consider the example in Fig. 4, which has $M = 3$ strips and a ground plane. Cases of this sort call for a capacitance matrix of order $N = M$, and for this example

$$\begin{bmatrix} C_{11} & C_{12} & C_{13} \\ C_{21} & C_{22} & C_{23} \\ C_{31} & C_{32} & C_{33} \end{bmatrix} \begin{bmatrix} V_1 \\ V_2 \\ V_3 \end{bmatrix} = \begin{bmatrix} q_{11} \\ q_{12} \\ q_{13} \end{bmatrix}. \quad (19)$$

(For cases without a ground plane, to be discussed in the next section, the matrix will be of order $N = M - 1$.) Here the subscripts t on the q_{tn} are meant to imply the *total* charge per unit length on conductor n (in contrast to q in (6), which is the charge per unit length on only one face of a conductor). We can solve for the capacitances in column p of equations such as (19) by applying a potential V_p to conductor p and setting the potentials of all other conductors to zero. Then

$$C_{np} = \frac{q_{tn}}{V_p} \Big|_{\text{All } V_j = 0 \text{ except for } j = p} \quad (20)$$

which for a given value of p is used to obtain C_{np} values for $n = 1$ to N . The actual computations are accomplished by solving (18b) with

$$\begin{aligned} v_k &= V_p & \text{for all } z_k \text{ on conductor } p \\ v_k &= 0 & \text{for all other } z_k \end{aligned} \quad (21)$$

in order to get the Q_m . Then in order to get q_m for conductor n we use

$$q_m = \epsilon_0 \sum Q_m \quad (22)$$

summed over all sides m on conductor n . (The sum above will have four terms if basis functions are used for all four sides of the conductor n .) This is repeated so as to compute the total charge induced on each of all N strips by the voltage on strip p with all other strips grounded. Then the C_{np} are obtained using (20). In order to compute the N^2 capacitance coefficients (18b) is solved N times, each time with a voltage V_p applied to a different conductor with all other conductors grounded.

VI. CALCULATION OF CAPACITANCE MATRICES WHEN A GROUND PLANE IS NOT PRESENT

In many digital situations the spacing between conductors is small compared with the thickness of the substrate, and the conductors are driven by devices connected between them on the surface of the substrate. In such situations even though the bottom of the substrate may be metallized it will have negligible effect, and the thickness of the substrate can be viewed as infinite. Also, since the conductors are driven by devices connected between them on the surface *the total net charge on the conductors must add to zero*. The examples in Figs. 2 and 3 are both of this sort. In the case of Fig. 2 the symmetry of the geometry and applied voltages guarantees that the total charge will add to zero. However, in the asymmetrical case in Fig. 3 additional steps are necessary to ensure zero net charge on the conductors so that the capacitance between the conductors will be computed correctly. The procedure will be explained in terms of a somewhat more general example.

Fig. 5 shows a case of three conductors on a semi-infinite dielectric substrate. In this case conductor no. 0 will be viewed as the "reference" or "return" conductor and the voltages V_1 and V_2 on lines no. 1 and no. 2, respectively, are measured with respect to the potential on line no. 0. The charges on lines 1 and 2 caused by V_1 and V_2 are q_{11} and q_{12} , and these must always be balanced by charge q_{10} on line no. 0. It will be necessary for us to take a special step in order to enforce this charge-balance condition. This charge-balance constraint has the effect of uniquely fixing the potential of the strips with respect to infinity. If we only fixed V_1 and V_2 defined in Fig. 5 the values of q_{11} and q_{12} would not be unique because the potential of the three strips with respect to infinity would still be arbitrary. Note that enforcing charge balance was not necessary for the cases treated in Section V, which had ground planes, because the presence of a plane at zero potential ensures that the charges on the strips plus the charges on their images will always add to zero.

To treat a case which has no ground plane, such as the case in Fig. 5, we use (18b) M times (where M is the total number of strips), each time with different potentials applied to the strips. We first solve the equations using potential $v_k = V$ (1 V for convenience) at all points on all strips. This results in charges having the same sign on all strips with equal and opposite charges at infinity. In this way the charge-voltage relationship with respect to infinity (i.e., ground) is established. We will designate the resulting total charges on the strips obtained with the aid of (22) as q'_m . Next in order to compute the capacitances in column p of the capacitance matrix we apply a voltage V_p to all points on conductor p (where p is not zero) and zero voltage to all points on all the other conductors including no. 0. Solving (18b) and (22) leads to another set of M charges q''_m with $n = 0$ to $N = M - 1$. To enforce charge balance we then solve for α_p in

$$\sum_{n=0}^N q'_m + \alpha_p \sum_{n=0}^N q''_m = 0. \quad (23)$$

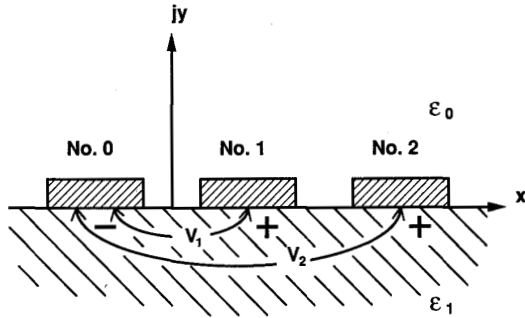


Fig. 5. Three transmission-line conductors on a semi-infinite dielectric substrate. Here the voltages on lines 1 and 2 are referred to line 0.

The resulting corrected charges on strips 1 to $N = M - 1$ are then obtained using

$$q_{in} = q'_{in} + \alpha_p q''_{in}, \quad (24)$$

and the values for column p of the capacitance matrix are then obtained using (20). This process is repeated for $p = 1$ to N applying a voltage V_p to conductor p and zero voltage to all other conductors of the structure in order to obtain the elements in all $N = M - 1$ columns of the capacitance matrix. It is of interest to note that if α_p had been known ahead of time the charges obtained by (24) could have been obtained immediately from (18b) if a voltage $V_p + \alpha_p V$ had been applied to conductor p and a voltage $\alpha_p V$ was applied to all the other conductors.

VII. ADDITION OF ANOTHER DIELECTRIC OR METAL INTERFACE

The examples in Figs. 3, 4, and 5, which involve only one dielectric interface or one ground plane with no dielectric interface, require only one set of images. However, a case such as that in Fig. 6, which has two dielectric interfaces, cases having one dielectric and one metal interface, and cases having two metal interfaces all theoretically call for an infinite number of images [9]. However, we have found that if we truncate a sequence of images and then adjust the charge of the last image in the truncated sequence so that the total net charge of the truncated sequence is the same as that for the infinite sequence, good accuracy can be obtained using relatively few images. Also, the smaller the change in dielectric constant at one or both interfaces the smaller the number of images that will be required to give good accuracy. Of course, since the images of a charge are included in its basis function, the number of images used does not affect the number of complete basis functions needed or the size of the matrix that must be inverted to find the charges.

For cases such as that in Fig. 6 we define two image coefficients:

$$K_1 = \frac{\epsilon_0 - \epsilon_1}{\epsilon_0 + \epsilon_1} \quad K_2 = \frac{\epsilon_1 - \epsilon_2}{\epsilon_1 + \epsilon_2}. \quad (25)$$

Either the upper region or the lower region (or both) can be defined as metal by allowing $\epsilon_0 \rightarrow \infty$ or $\epsilon_2 \rightarrow \infty$. For

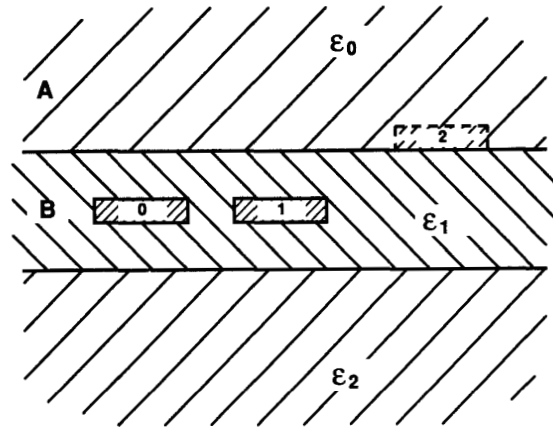


Fig. 6. Transmission-line conductors in multiple dielectrics.

brevity we will construct the basis functions with images as a function of $f(z, b, w)$, where $f(z, b, w)$ is the function in (2b), (4b), (12), or (13) depending on whether the basis function is for a horizontal even- or odd-charge distribution or for a vertical even- or odd-charge distribution, respectively. As previously discussed, b is a complex number which defines the location of the center of the charge distribution and w defines its width. Note that the upper region in Fig. 6 is marked A while the dielectric layer of dielectric constant ϵ_1 is marked B . The images required are different depending on whether the charge and the point for observing the potential are both in region A , both in region B , or the charge is in one region and the observation point in the other. To identify the equations for the four possibilities we will use two letters, the first indicating the region of the observation point and the second the region of the charge. Thus, $AA(z, b, w)$ will apply when the observation point and charge are both in region A while the equation for $AB(z, b, w)$ will apply when the observation point is in region A but the charge is in region B . The equations covering the four possible situations with reference to regions A and B in Fig. 6 are

$$\begin{aligned} AA(z, b, w) = & f(z, b, w) + K_1 f(\bar{z} + 2jh, b, w) \\ & + K_2 (1 - K_1^2) \left[\sum_{n=0}^{D-1} (-K_1 K_2)^n \right. \\ & \cdot f(\bar{z} - 2jnh, b, w) \\ & \left. + a_1 f(\bar{z} - 2jDh, b, w) \right] \quad (26) \end{aligned}$$

$$\begin{aligned} AB(z, b, w) = & (1 + K_1) \left[\sum_{n=0}^{D-1} (-K_1 K_2)^n \right. \\ & \cdot [f(z + 2jnh, b, w) \\ & + K_2 f(\bar{z} - 2jnh, b, w)] \\ & + a_1 [f(z + 2jDh, b, w) \\ & \left. + K_2 f(\bar{z} - 2jDh, b, w)] \right] \quad (27) \end{aligned}$$

$$\begin{aligned}
BA(z, b, w) &= \frac{(1 - K_1)}{\epsilon_1/\epsilon_0} \left[\sum_{n=0}^{D-1} (-K_1 K_2)^n \right. \\
&\quad \cdot [f(z - 2jnh, b, w) \\
&\quad + K_2 f(\bar{z} - 2jnh, b, w)] \\
&\quad + a_1 [f(z - 2jDh, b, w) \\
&\quad \left. + K_2 f(\bar{z} - 2jDh, b, w)] \right] \quad (28) \\
BB(z, b, w) &= \frac{1}{\epsilon_1/\epsilon_0} \sum_{n=0}^{D-1} (-K_1 K_2)^n [f(z + 2jnh, b, w) \\
&\quad + K_2 f(\bar{z} - 2jnh, b, w)] \\
&\quad + \frac{a_1}{\epsilon_1/\epsilon_0} [f(z + 2jDh, b, w) \\
&\quad + K_2 f(\bar{z} - 2jDh, b, w)] \\
&\quad - \frac{K_1}{\epsilon_1/\epsilon_0} \sum_{n=1}^{D-1} (-K_1 K_2)^{n-1} [f(\bar{z} + 2jnh, b, w) \\
&\quad + K_2 f(z - 2jnh, b, w)] \\
&\quad + \frac{a_1}{K_2 \epsilon_1/\epsilon_0} [f(\bar{z} + 2jDh, b, w) \\
&\quad + K_2 f(z - 2jDh, b, w)] \quad (29)
\end{aligned}$$

where

$$a_1 = \frac{(-K_1 K_2)^D}{1 + K_1 K_2}. \quad (30)$$

In these equations D is the number of images (or pairs of images) to be included. These equations were derived largely using the methods in [9], but as previously mentioned, the strength of the last image of each type has been adjusted to give the same total net charge for the truncated array as for the infinite array of images.

Some experimentation suggests that a useful guide in fixing a minimum value for D is

$$D = 1 + \lceil (\text{Integer}) \geq -1.4 / \log |K_1 K_2| \rceil. \quad (31)$$

Thus for a structure with relative dielectric constants $\epsilon_{r0} = 1$, $\epsilon_{r1} = 6$, and $\epsilon_{r2} = 13$, (31) calls for $D = 4$. For the case of microstrip we use $\epsilon_{r2} = \infty$ for the ground plane (so $K_2 = -1$), so if $\epsilon_{r0} = 1$ and $\epsilon_{r1} = 2$, again a minimum of $D = 4$ is recommended. However, for microstrip with $\epsilon_{r1} = 13$, a minimum D of 21 is called for. These values of D are adequate for most situations, but for some cases larger values of D will be desired for reasons to be discussed in Section X.

To illustrate the use of the above equations, suppose we wished to generate a matrix element analogous to P_{km}^o in (16a) for an odd, horizontal charge distribution located in region B of Fig. 6 with the observation point also in region B (as would be the case for obtaining the distributed capacitance for the two lower bars shown. Then

P_{km}^o would be given by (29) with (4b) inserted for $f(z, b, w)$. The potentials arising from even and odd charge basis-function distributions on all the conductor faces are determined analogously using (2b), (4b), (12), or (13) for $f(z, b, w)$. In this manner the matrix in (18b) is constructed and the solution proceeds as discussed in the preceding sections. Note that if the strips are all in the same dielectric region only (26) or (29) will be required for constructing the matrix in (18b). However, if one of the strips is in a different region, as suggested by strip no. 2 in Fig. 6, then the four equations (26) through (29) will all become involved.

VIII. THE CASE OF STRIPLINE

A special situation arises in the case of the stripline structure in Fig. 7. The top and bottom ground planes can be simulated by setting $\epsilon_0 = \epsilon_2 = \infty$. Then $K_1 = 1$, $K_2 = -1$, and there are an infinite number of images, all with unit positive or negative amplitude (instead of with declining amplitudes as in all of the previous cases). Because of this, this problem needs a large number of images (i.e., hundreds) for high accuracy unless some special modifications are made in the truncated image arrays. For convenience, and to reduce the number of images needed to obtain good accuracy, we recast (29) in the form

$$\begin{aligned}
BB(z, b, w)_{SL} &= \sum_{n=0}^{D-1} [f(z + j2nh, b, w) \\
&\quad - f(\bar{z} - j2nh, b, w)] \\
&\quad + 0.5(R_b^{e,o} + 1)f(z + j2Dh, b, w) \\
&\quad - 0.5R_b^{e,o}f(\bar{z} - j2Dh, b, w) \\
&\quad - \sum_{n=1}^D [f(\bar{z} + j2nh, b, w) \\
&\quad - f(z - j2nh, b, w)] \\
&\quad + 0.5(R_t^{e,o} - 1)f(z - j2Dh, b, w) \\
&\quad - 0.5R_t^{e,o}f(\bar{z} + j2(D+1)h, b, w) \quad (32)
\end{aligned}$$

where R_t^e and R_t^o are the fraction of the total flux caused by a charge distribution $f(z, b, w)$ that terminates on the top plate for even and odd charge distributions, respectively, and R_b^e and R_b^o are the corresponding fractions of the flux that terminate on the bottom plate. We note that

$$R_b^{e,o} = 1 - R_t^{e,o} \quad (33)$$

and that if $f(z, b, w)$ is symmetrically placed with respect to the ground planes all the R 's will be 0.5.

The first summation in (32) represents the source charge plus all its images below the lower ground plane except those involving charge-balance corrections. The second summation includes all images above the upper ground plane except those involved in charge-balance corrections. Since the source function is defined with unit positive amplitude, if the source-charge function is centered

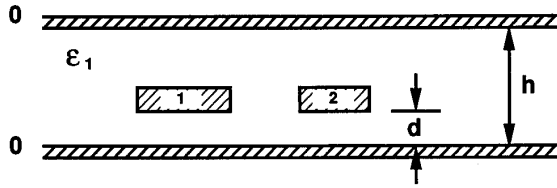


Fig. 7. An asymmetrical pair of striplines analyzed in Example 6.

between the ground planes we must provide a net, negative, half-unit amplitude in both the upper and lower ground-plane regions to provide charge balance. There are at least two simple ways to accomplish this. One is to use a truncated array of images with alternating positive and negative unit amplitudes so they have zero net charge and then add on an additional image with -0.5 amplitude. Another approach is to simply cut the amplitude of the last positive unit image in the upper and lower image array in half, again leaving a net charge of -0.5 in each of the two arrays. In some examples we have tried using $D = 21$, these two approaches gave somewhat different results with errors in opposite directions. We further found that we obtained considerably improved results while using a relatively small number of images (such as $D = 21$) if we used the average of the two approaches. This was done in the third and fourth, and the seventh and eighth lines of (32).

Of course, if the source charge $f(z, b, w)$ is asymmetrically positioned between the ground planes more of the flux lines will terminate on one plane than the other, and the R factors discussed above were introduced for that reason. If $f(z, b, w)$ is (2b) or (4b), which give the potentials for horizontal charge distributions, we use the approximations

$$R_t^e = \frac{H_e(z_{hb}, b, w)}{H_e(z_{hb}, b, w) + H_e(z_{ht}, b, w)} \quad (34)$$

and

$$R_t^o = \frac{|H_o(z_{ht}, b, w)|}{|H_o(z_{hb}, b, w)| + |H_o(z_{ht}, b, w)|} \quad (35)$$

where

$$z_{hb} = \text{Re } b + (rh)w \quad (36a)$$

$$z_{ht} = z_{hb} + jh. \quad (36b)$$

If $f(z, b, w)$ is (12) or (13) for a vertical charge distribution we use the approximations

$$R_t^e = \frac{U_e(z_{vb}, b, w)}{U_e(z_{vb}, b, w) + U_e(z_{vt}, b, w)} \quad (37)$$

$$R_t^o = \frac{|U_o(z_{vt}, b, w)|}{|U_o(z_{vb}, b, w)| + |U_o(z_{vt}, b, w)|} \quad (38)$$

where

$$z_{vb} = \text{Re } b \quad (39a)$$

$$z_{vt} = z_{vb} + jh. \quad (39b)$$

The different definitions for the even and odd cases are needed because using our even potential functions the magnitude of the potential becomes larger as you get further from the source while for our odd potential functions the magnitude of the potential becomes smaller as you move from the source, and these properties affect the charge-division approximations in (34) through (39b). Inclusion of these charge-division factors in (32) gives a considerable improvement in the results for asymmetrical cases.

It should be noted that since ϵ_0 was made to be infinite to get (32) from (29), in this case the charge normalizations in (6) and (22) must use ϵ_1 , the dielectric constant for the region between the conductors, rather than ϵ_0 .

IX. CALCULATION OF INDUCTANCE MATRICES

As is well known [2], for TEM-mode operation the inductance matrix is easily obtained from the capacitance matrix $[C^0]$ which is computed for the same conductors but with all dielectric materials assumed to be replaced by air. The inductance matrix is then

$$[L] = \mu_0 \epsilon_0 [C^0]^{-1} \quad (40)$$

where ϵ_0 and μ_0 are the electric permittivity and magnetic permeability of free space.

X. SOME FURTHER EXAMPLES

Example 1, previously discussed, consisted of two infinitesimally thick symmetrical coplanar strips as shown in Fig. 2, and various results were listed in Table I along with the percentage errors compared with the results obtained from an exact conformal mapping solution. As can be seen, excellent agreement compared with the exact values were obtained.

In all of the following examples results computed using the Ansoft finite-element program [5] were used as a basis for comparison. In the Ansoft reference calculations a fast computer utilizing thousands of mesh triangles was used for each example, and the results are believed to be highly accurate. However, since we do not know the absolute accuracy of the reference calculations we will refer to the percentage difference between the results obtained from our program based on the methods of this paper compared with the Ansoft results. In order to obtain relative running times for the various examples using our program we ran the examples using our program on a 1985-vintage, Compaq, IBM-PC-compatible computer. (When run on a Sun 4 computer our program usually appeared to give practically instantaneous results.)

As Example 2, let us consider the case of three coplanar thick strips on a semi-infinite substrate, shown in Fig. 5. To accommodate the dielectric substrate, single image charges are used in the basis functions as in (15a) to (16b). We used $rh = rv = 0.8$ for fixing the potential-matching points since, as previously mentioned, we have found these values to be particularly good when no ground plane is present. Also, since the voltages on strips 1 and 2 are

referred to strip 0, charge balance must be enforced and the methods in Section VI were used. The dimensions used for this example were $w_0 = 4$, $w_1 = w_2 = 3$, $t_0 = t_1 = t_2 = 1$, and $s_{01} = s_{12} = 2$, where the w_k and t_k are the width and thickness of strip k , and $s_{k,k+1}$ is the spacing between strips k and $k + 1$. (We will use this notation also for all the following examples.) Using relative dielectric constants $\epsilon_{r0} = 1$ and $\epsilon_{r1} = 2$ we obtained

$$[C] = \begin{bmatrix} 46.20 & -22.63 \\ -22.64 & 31.87 \end{bmatrix}, \begin{bmatrix} 0.06 & -0.06 \\ 0.01 & -0.01 \end{bmatrix} \% \quad (41)$$

where the capacitance values in the matrix on the left are in pF/m, and the matrix on the right gives the percentage difference between our values and the values given by the Ansoft program. With $\epsilon_{r1} = 13$ we got

$$[C] = \begin{bmatrix} 179.46 & -87.35 \\ -87.44 & 128.44 \end{bmatrix}, \begin{bmatrix} 0.24 & 0.10 \\ 0.20 & 0.10 \end{bmatrix} \% \quad (42)$$

The percentage-difference matrices on the right for both of these cases show the agreement between our results and the Ansoft results to be excellent. The running time for these examples on the Compaq computer was 8 s each. At the suggestion of one of the reviewers of this paper we ran an additional case similar to that in Fig. 5 with $w_0 = 4$, $w_1 = w_2 = 3$, $t_0 = t_1 = t_2 = 3$, $s_{01} = s_{12} = 1$, $\epsilon_{r0} = 1$, and $\epsilon_{r1} = 2$. The differences between the capacitance coefficients obtained from our program compared with those obtained from the Ansoft program ranged from -0.34 to -0.53% using matching parameters $rh = 0.8$ and $rv = 0.67$. This is an unusual example in that the gaps between the strips are proportioned to be narrow and tall. Using $rv = 0.67$ for the vertical faces was found to give several percent better accuracy than using $rv = 0.8$. The reason for this is probably the same as that which causes $rh = 0.67$ to be a better choice for the horizontal faces when there is a horizontal ground plane nearby. In this present example, which had no ground plane, using either $rh = 0.8$ or $rh = 0.67$ for the horizontal faces gave about the same accuracy, although the results for the former were slightly smaller than the Ansoft results while those for the latter were slightly larger.

As Example 3 we will use the same configuration of strips as for Example 2 but instead of using a semi-infinite substrate we will make the substrate $h = 2$ thick with a ground plane on the bottom as sketched in Fig. 8. In this case the strip voltages are referred to the ground plane so the methods in Section V are used. Because of the presence of both a dielectric and a metal interface there are, in theory, an infinite number of images. These are approximated using basis functions analogous to (15a) to (16b) constructed from the source charge plus a truncated set of images defined by (26). In this case $\epsilon_2 = \infty$ is used to define the metal ground plane so $K_2 = -1$. Here we used $rh = 0.67$ and $rv = 0.8$ because, as previously mentioned, these appear to be particularly good for fixing the match points when one or more ground planes are present.

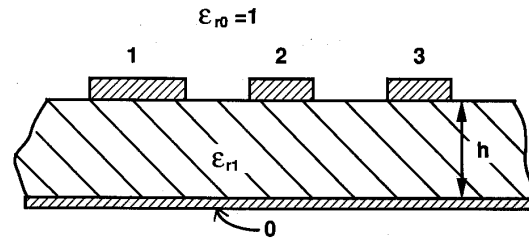


Fig. 8. Transmission lines analyzed in Example 3.

For the case of $\epsilon_{r0} = 1$ and $\epsilon_{r1} = 2$ we obtained, using $D = 4$ as called for by (31),

$$[C] = \begin{bmatrix} 73.08 & -11.71 & -1.08 \\ -11.72 & 66.53 & -11.46 \\ -1.08 & -11.46 & 63.38 \end{bmatrix}, \begin{bmatrix} -0.16 & -0.77 & -0.40 \\ -0.79 & 0.04 & -0.65 \\ -0.38 & -0.65 & 0.03 \end{bmatrix} \% \quad (43)$$

where the running time was 9 s. Again the agreement with Ansoft results is excellent. Note that the matrix is third order because now there are three independent voltages.

If we modify this example so that $\epsilon_{r1} = 13$, then (31) calls for $D = 21$ images. If this example had only the two strips on the left in Fig. 8 there would be no advantage in using a D larger than that. However, we have found that in cases such as this, where there are an appreciable number of images called for by (31), if any of the strips have much separation it is better to use additional images. This is apparently because widely separated strips obtain an oblique view of the images and are more sensitive to the fact that the array of images has been truncated. In this case we used $D = 41$. (However, $D = 31$ gives nearly the same results. If there is doubt about the value of D to use increasing values of D can be tried until further increase gives negligible change in the answers.) We obtained

$$[C] = \begin{bmatrix} 357.4 & -24.79 & -1.03 \\ -24.47 & 302.6 & -24.31 \\ -1.03 & -24.31 & 299.0 \end{bmatrix}, \begin{bmatrix} -0.26 & 0.13 & -3.06 \\ 1.42 & -0.60 & 1.89 \\ -2.87 & 1.88 & -0.36 \end{bmatrix} \% \quad (44)$$

in a running time of 43 s. Note the principal-diagonal percentage differences with respect to the Ansoft results are very small, though the differences for the mutual capacitances between the most remote conductors are around 3%. But even in these cases the *absolute* differences are extremely small because the mutual capacitances between the remote strips are themselves only about 0.3% as large as the self-capacitances. Thus the larger *percentage* dif-

ferences compared with the Ansoft results for these relatively small mutual capacitances will usually be of negligible engineering importance.

In the previous two cases we used $rh = 0.67$ and $rv = 0.8$, which we have found to be advantageous if a ground plane is present. A possible exception to this general recommendation is that if the ground plane is remote it will be better to go back to $rh = rv = 0.8$, as for no ground plane. (In terms of ordinary engineering accuracy requirements the choice between $rh = 0.67$ and 0.8 is not critical.) Another phenomenon that we have observed is that if the gaps between strips are so small that, say, $s/t < 1$ (where s and t are as defined for Example 2) it appears to be preferable to use $rh = 0.8$ instead of 0.67 even if one or more ground planes are present. This may be because the fields are so concentrated around the gap that the significance of the ground plane is reduced.

As a fourth example, consider the GaAs substrate ($\epsilon_{r2} = 13$) in Fig. 9, which has three strips with a cover layer having $\epsilon_{r1} = 6$. The voltage of strips 1 and 2 is referred to strip 0, and the dimensions are $w_0 = 4$, $w_1 = w_2 = 2$, $t_0 = t_1 = t_2 = 0.6$, $s_{01} = s_{12} = 2$, and $h = 1.2$. Since there is no ground plane we use $rh = rv = 0.8$, and, using (31), $D = 4$ was used. In a run time of 26 s our program yielded

$$[C] = \begin{bmatrix} 211.3 & -100.9 \\ -101.11 & 147.4 \end{bmatrix}, \begin{bmatrix} 0.23 & 0.05 \\ -0.12 & 0.05 \end{bmatrix} \% \quad (45)$$

again with very small percentage differences with respect to the Ansoft results.

In Fig. 10 is shown a fifth example, which is more complex to program than the previous examples because it requires the use of all four of the equations (26) to (29) since some of the source and observation points are in different media. The dimensions used were $w_0 = w_1 = 2$, $t_0 = t_1 = 0.6$, $s_{01} = 2$, and $h = 1.2$. For reasons previously discussed, $rh = rv = 0.8$ and $D = 4$ were used. In this case there is only one capacitance to be considered since the voltage on strip 1 is referred to strip 0. In a running time of 7 s the value $C = 82.33$ pF/m was obtained, which is within -0.37% of the Ansoft results.

We will use the stripline situation in Fig. 7 as a sixth example. In this case let $\epsilon_{r1} = 1$, and the dimensions are taken to be $w_1 = 4$, $w_2 = 2$, $t_1 = t_2 = 1$, $s_{12} = 2$, $h = 6$, and $d = 1.5$, making the structure asymmetric in both the horizontal and the vertical direction. Here the methods of Section VIII were used with $D = 21$ (a value we happened to have used in testing the methods described there), and $rh = 0.67$ with $rv = 0.8$ were used because of the presence of ground planes. The program gave in 33 s the results

$$[C] = \begin{bmatrix} 59.77 & -7.16 \\ -7.20 & 42.92 \end{bmatrix}, \begin{bmatrix} -0.47 & -0.10 \\ -0.66 & -0.14 \end{bmatrix} \% \quad (46)$$

which are in good agreement with Ansoft results.

As a seventh and final example let us endeavor to compare the performance of the methods in this paper with

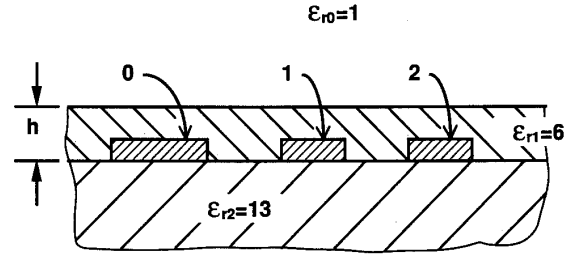


Fig. 9. Transmission lines analyzed in Example 4.

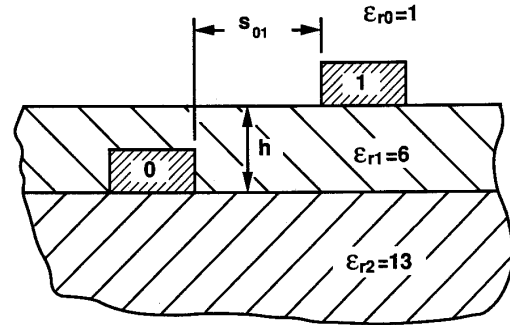


Fig. 10. The cross section of the conductors of a transmission line analyzed in Example 5.

methods such as those in [2], which use a sizable number of pulse basis functions in order to approximate the charge functions. This is done most easily using the program [3] which is written for IBM compatible PC's and uses the methods in [2]. The example chosen is the same as that in Example 3 and Fig. 8 with $\epsilon_{r1} = 13$ except that the right strip was removed, making it only a two-strip example and h was increased from 2 to 3. Our program using $D = 21$, as called for by (31), took 10 s on the Compaq PC and the differences for C_{11} , C_{12} , C_{21} , and C_{22} compared with the Ansoft results were 0.11, 0.20, 0.82, and 0.01%, respectively. When program [3] was used to solve the same problem with the same machine we used 140 "nodes," which gives the largest number of basis functions available in that particular program. It is of interest to note that [2] and [3] use pulse charge basis functions for the metal and also for the bound charge at dielectric interfaces, thus eliminating the need to use images for dielectric interfaces. In the present example with $\epsilon_{r1} = 13$ the bound charges are quite large. We used a program option where the ground plane was simulated using images (which we believe should be the most efficient for this problem). The running time was 6 min and 2 s, and the differences with respect to the Ansoft results were -2.35 , 2.78 , 3.22 , and -3.06% , respectively. For perspective it should be recalled that the methods of our paper are specialized to cases having rectangular or planar conductors, while the methods in [2] are completely general. Using the methods of [2] with sufficient basis functions it should be feasible to achieve almost any desired degree of accuracy for arbitrarily shaped conductors pro-

vided the required amount of computation is available and acceptable.

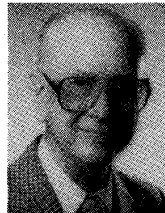
XI. CONCLUSIONS AND CLOSING REMARKS

A relatively simple, fast, and quite accurate technique has been presented for calculating the distributed capacitances and inductances of multiple, rectangular, or planar transmission lines. Particularly for cases where the conductors are all in the same dielectric, the required programming is quite simple, and it should be relatively easy for engineers to write subroutines for such computations for use in CAD programs. Also, the methods used require relatively little computational effort so that they can be readily implemented for machines as small as ordinary personal computers.

The methods described herein acquire their simplicity and speed as a result of using only two basis functions per face of the conductors in order to represent the charge. These charge basis functions are functions which are physically relevant to this application and happen to be ones from which the potentials are easily computed. How accurate the results will be in a given instance will, of course, depend on how accurately the given basis functions can approximate the actual charge distribution. Thus, one would expect that the charge distributions in parts (b) and (c) of Fig. 1 could not represent situations very accurately where the actual charge is much more sharply concentrated at one or both edges of the conductor than is represented by the basis function. Yet as is indicated in the first example and Table I, the method gives very accurate results for the capacitance between the strips in Fig. 2 even when the gap between the strips is as small as $s = w/10$ (which should give quite sharp charge concentration at the inner edges of the strips). The approximations are surprisingly insensitive in this regard. (Similar results have been obtained for finite-thickness strips having small gaps.) However, when applying these methods to unusual geometries the actual physical nature of the approximations being utilized should be kept in mind so as not to misuse them. For common geometries, such as in our examples, the basis functions used appear to work remarkably well.

REFERENCES

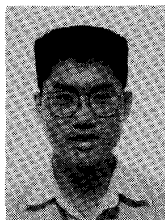
- [1] W. T. Weeks, "Calculation of coefficients of capacitance of multiconductor transmission lines in the presence of a dielectric interface," *IEEE Trans. Microwave Theory Tech.*, vol. MTT-18, pp. 35-43, Jan. 1970.
- [2] C. Wei, R. F. Harrington, J. R. Mautz, and T. K. Sarkar, "Multiconductor transmission lines in multilayered dielectric media," *IEEE Trans. Microwave Theory Tech.*, vol. MTT-32, pp. 439-450, Apr. 1984.
- [3] A. Djordjevic *et al.*, *Matrix Parameters for Multiconductor Transmission Lines: Software and User's Manual*. Norwood, MA: Artech House, 1989.
- [4] Z. Pantic and R. Mittra, "Quasi-TEM analysis of microwave transmission lines by the finite-element method," *IEEE Trans. Microwave Theory Tech.*, vol. MTT-34, pp. 1096-1103, Nov. 1986.
- [5] Finite-element programs "Meshmaker" and "Electrostat," Ansoft Corp., Pittsburgh, PA, 1988.
- [6] P. Silvester, *Modern Electromagnetic Fields*. Englewood Cliffs, NJ: Prentice-Hall, 1968, pp. 101-103.
- [7] R. Mittra and S. W. Lee, *Analytical Techniques in the Theory of Guided Waves*. New York: Macmillan, 1971, pp. 10 and 11.
- [8] S. B. Cohn, "Shielded coupled-strip transmission lines," *IRE Trans. Microwave Theory Tech.*, vol. MTT-3, pp. 29-38, Oct. 1955.
- [9] P. Silvester, "TEM wave properties of microstrip transmission lines," *Proc. Inst. Elec. Eng. (London)*, vol. 115, pp. 43-48, Jan. 1968.



George L. Matthaei (S'49-A'52-M'57-F'65-LF'89) received the B.S. degree from the University of Washington in 1948 and the Ph.D. degree from Stanford University in 1952.

From 1951 to 1955, he was on the faculty of the University of California, Berkeley, where he was an Assistant Professor, and his specialty was network synthesis. From 1955 to 1958, he was engaged in system analysis and microwave component research at the Ramo-Wooldrige Corporation. From 1958 to 1964, he was at Stanford Research Institute, where he was engaged in microwave device research and became Manager of the Electromagnetic Techniques Laboratory in 1962. In July 1964, he joined the Department of Electrical Engineering at the University of California, Santa Barbara, where he was a Professor, and in July 1991 he became a Professor Emeritus. He is also a consultant. Dr. Matthaei is the author of numerous papers, coauthor of the book *Microwave Filters, Impedance-Matching Networks and Coupling Structures*, and a contributor to several other books. His current interests are in the areas of crosstalk and wave effects in digital circuits, and microwave and millimeter-wave passive and active circuits.

Dr. Matthaei is a member of Tau Beta Pi, Sigma Xi, and Eta Kappa Nu. He was a winner of the 1961 Microwave Prize of the IEEE MTT Group. In 1984 he received an IEEE Centennial Medal and in 1986 the Microwave Career Award of the IEEE Microwave Theory and Techniques Society.



Gilbert C. Chinn was born in Hong Kong in 1966. He received the B.S. degree from the University of California, Los Angeles, in 1988 and is currently pursuing work toward the M.S. degree at the University of California, Santa Barbara. His current interests are in the modeling of high speed digital interconnects, general relatively, and jazz/classical guitar.



Charles H. Plott (S'87-M'89) received the B.S. degree in electrical engineering and the B.A. degree in economics/mathematics in March 1989 from the University of California, Santa Barbara.

In 1989, he joined Hewlett-Packard's Network Measurements Division as a Product Marketing Engineer, where he has been working with HP's Microwave Design System and High Frequency Structure Simulator software products. He is also currently working toward the M.S. degree in electrical engineering at Stanford University.



Nadir Dagli (S'77-M'86) was born in Ankara, Turkey. He received the B.S. and M.S. degrees in electrical engineering from the Middle East Technical University, Ankara, Turkey, in 1976 and 1979, respectively, and the Ph.D. degree, also in electrical engineering, from the Massachusetts Institute of Technology, Cambridge, in 1986. During his Ph.D. research he worked on the design, fabrication, and modeling of guided-wave integrated optical components in III-V compound semiconductors. He also worked on III-V mate-

rials preparation by LPE and the modeling and analysis of heterojunction bipolar transistor for microwave and millimeter-wave applications.

He is currently an Assistant Professor at the University of California, Santa Barbara. His current interests are the design, fabrication, and modeling of guided-wave components for optical integrated circuits, solid-state microwave and millimeter-wave devices, electron waveguides, and novel quantum interference devices based on electron waveguides.

Dr. Dagli was awarded NATO science and IBM predoctoral fellowships during his graduate studies. He was the recipient of the 1990 UCSB Alumni Distinguished Teaching Award and of a 1990 UC Regents Junior Faculty Fellowship.